Laboratory modeling of magnetized accretion dynamics

G. Revet[1,2], D. P. Higginson[1], J. Béard[3], M. Bleicher[4], K. Burdonov[2], M. Borghesi[7], S. N. Chen[1], D. Khagani[5], B. Khiar[6], K. Naughton[7], S. Pikuz[8,10], C. Riconda[1], R. Riquier[1], A. Soloviev[2], T. Vinci[1], O. Willi[4], O. Portugall[3], H. Pépin[9], A. Ciardi[6], J. Fuchs[1,2]

[1]*LULI, École Polytechnique, CNRS, CEA, UPMC, 91128 Palaiseau, France*

[2]*IAP-RAS, Nizhny Novgorod, Russia*

[3]*LNCMI, UPR 3228, CNRS-UFJ-UPS-INSA, 31400 Toulouse, France*

[4]*Institut für Laser-und Plasmaphysik Heinrich Heine Universität Düsseldorf, Germany*

[5]*GSI Helmholtzzentrum für Schwerionenforschung GmbH, 64291 Darmstadt, Germany*

[6]*LERMA, Observatoire de Paris, PSL Research University, CNRS, Sorbonne University, UPMC Univ. Paris 06, F-75005, Paris, France*

[7]*School of Mathematics and Physics, The Queen's University of Belfast, Belfast, UK*

[8]*Joint Institute for High Temperatures RAS, Moscow 125412, Russia*

[9]*INRS-EMT, Varennes, Québec, Canada*

[10]*National Research Nuclear University MEPhI, 115409 Moscow, Russian Federation*

1. Introduction

The dynamics of matter accretion in Young Stellar Objects (YSO) is currently a subject of debate and active astrophysical research. Matter (10^{-11}–10^{-13} g.cm^{-3}) can be extracted from the accretion disk and falls down whilst imbedded in a strong magnetic field (B ~kG) at the free fall velocity (100 – 500 km.s^{-1}) onto the stellar surface, in the form of well collimated plasma columns following the magnetic field lines [1,2]. The shock resulting from the impact of these plasma columns onto the stellar surface heat up the infalling flow. Previous experiments have attempted to reproduce accretion shocks in the laboratory using shock-tube configurations. This however created unwanted edge-constraints due the tube walls, and the experiment suffered from a lack of magnetic field [3].

In this paper, we report on an experimental setup which allows us to investigate the accretion dynamics in a magnetized environment. We detail the characteristics of the collimated magnetized plasma jet that is launched onto an obstacle, as well as those of the obstacle before being impacted by the jet. In the light of these parameters, we discuss of the scaling between the astrophysical situation and our laboratory experiment.

2. Experimental setup

This experiment was performed at the ELFIE facility, at Ecole Polytechnique (France), using a chirped laser pulse delivering 40 J of energy within a 0.6 ns pulse duration at 1ω (λ = 1057 nm), leading to $I_{max} = 4.5 \times 10^{12}\ W/cm^2$. This laser pulse is used to irradiate a target in the center of a high-current Helmholtz coil, constructed at the Laboratoire National des Champs

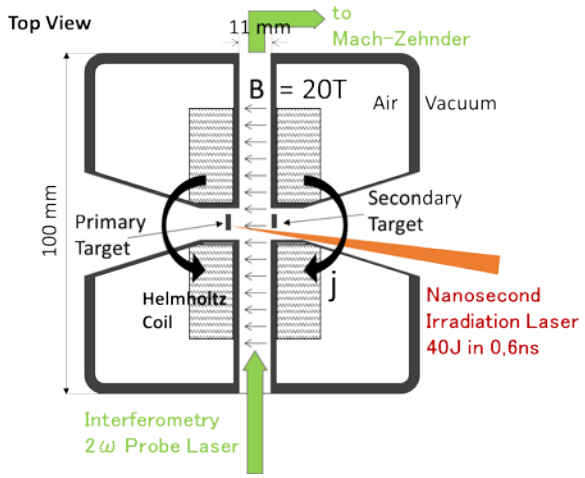

Fig. 1 : Top view of the experimental setup. Two targets (primary and secondary targets) look at each other. Their normal is parallel to the magnetic field lines generated by the Helmholtz coil. A longitudinal aperture allows the laser to irradiate the primary target. A radial aperture allows a clear line of sight to the plasma

Magnétiques Intenses (LNCMI, Toulouse, France). The collimated plasma jet originates from the laser interaction with this primary target (see section 3.1) and follows the magnetic field lines to finally hit a secondary Teflon target (CF_2). As shown in Fig. 1, two perpendicular apertures allow both targets to be inserted in the coil, and the laser to irradiate the jet source target, as well as a free line of sight for the diagnostics to access the plasma region. The coil is coupled to a 30 kJ/20 kV capacitor bank and delivers a 20 T pulsed (duration ~ 200 µs FWHM) magnetic field in the center of the coil. This magnetic field is homogeneous in the longitudinal and radial direction over, respectively 40 mm and 20 mm [4]. Thus, we can consider the magnetic field as constant across both space and time in comparison with the spatial and temporal scales of the plasma phenomena. Interferometric measurements of the plasma density use a compressed laser pulse (100 mJ in 350 fs, used at 2ω -λ = 528.5 nm-). Three other diagnostics are also used: a FSSR spectrometer yielding a 1D space-resolved measurement of the plasma temperature, a streak camera measuring in both time and 1D space the optical self-emission coming from the heated plasma, and an x-ray radiography diagnostic allowing to probe the accretion dynamics inside dense plasma region (i.e. close to the obstacle surface).

3. Accretion protagonists

3.1 Collimated jet

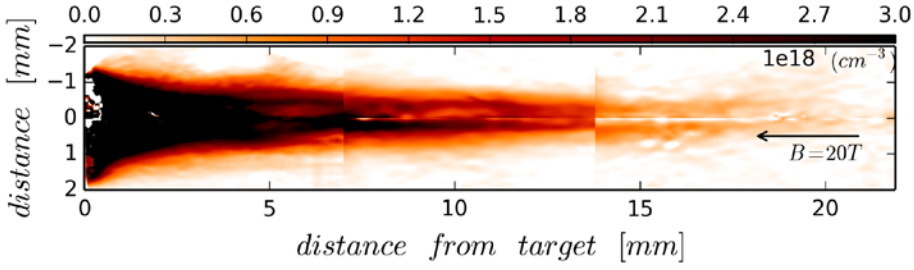

Fig. 2 : Electron density map of the magnetically collimated jet produced from the laser-irradiated target at 25 ns after laser irradiation, reconstructed from interferometry data via Abel inversion.

The presence of the strong magnetic field induces the collimation of the plasma into a narrow plasma jet with an aspect ratio >10, as shown in Fig. 2. This collimation mechanism is

studied in detailed in Ref [1,2]. The wide-angle flow expanding from the heated target, which is non-resistive, carries in its expansion motion the magnetic field lines and compresses them, forming a magnetic wall. Then, the particles are stopped, accumulated and heated at this point, forming a shock that draws the border of a plasma cavity, the center of which presents a lower magnetic pressure as well as a lower plasma density. The flow slides along the wall, forming at the tip of the cavity a conical shock. As a result of this shock and of a new compression of the magnetic field lines at the shock point, the flow is accelerated longitudinally in a very well collimated jet. Fig. 2 displays, at 25ns after laser irradiation, a typical jet resulting from this mechanism in our laser conditions and for a magnetic field of 20 T. To reconstruct this long jet image, the primary target was moved back inside the coil to allow the probing aperture to look at a farther region from the target surface.

The velocity of the jet can be deduced from the time taken by a certain amount of density to reach a certain distance from the source target. The temporal evolution of the density around the obstacle position shows that a density of $1.5 \times 10^{18}\ cm^{-3}$ is reached after 25 ns and stays quite constant over more than hundred nanoseconds. Tracking how much this $1.5 \times 10^{18}\ cm^{-3}$ density point travels along the coil, by scanning different timings of the probe, we find that the speed of the jet ~ 600 km.s^{-1}. Preliminary analysis of the FSSR spectrometer data gives a plasma temperature of tens of eV in the jet, at 3-4 mm from the target surface.

3.2 Obstacle

We observed that the obstacle is not completely cold when the jet reaches its surface. Indeed, the obstacle is heated by the x-ray emission coming from the interaction between the chirped laser pulse and the primary target. From the density profile of the obstacle measured in shots without magnetic field, and considering a standard self-similar expansion of the plasma, we can deduce a sound speed of 4.2 km.s^{-1}. Such a value of the sound speed is of course associated to a low temperature of the plasma (typically around 1 eV), and the gradient scale length of its expansion at the jet arrival time is $C_s \times t = 105\ \mu m$. Below this length, one can consider the density of the obstacle to be close to the solid density.

4. Scaling with astrophysical objects

In order to compare our laboratory accretion experiment to astrophysical cases, the table 1 displays some parameters, using the measured characteristics of the jet incident on the obstacle, and the characteristics of accretion in classical T Tauri stars (CTTS) [5, 6]. In this comparison, the astrophysical case is divided in two instances, for two different strengths of the

magnetic field, respectively at 5.10^{-3} T and 5.10^{-2} T, which allows us studying both a case where the magnetic pressure dominates compared to the kinetic pressure (i.e. the magnetic field is able to confine the plasma within the magnetic field lines) and the opposite case.

Although our laboratory case presents a higher temperature compared to the astrophysical case, the higher density of the laboratory jet allows it to reach a Mach number (>1) comparable to the one of the astrophysical configuration. Both cases present a magnetic Reynolds number >1, even if the laboratory presents a regime where R_m is only of a few units. The beta parameters suggests a more accurate correspondence of the laboratory case with the strong magnetic field astrophysical case.

5. Conclusion and perspectives

We have detailed a new experimental setup combining laser-produced plasmas and strong external magnetic fields in order to model accretion dynamics in the laboratory. Both the jet and the obstacle characteristics have been detailed; this configuration proves to be scalable to the astrophysical case in some regimes. The pivotal role played by the magnetic field in our experiment leads us to think that this experimental setup will be able to reproduce interesting effects regarding the dynamics of the accretion shock in relation with astrophysical cases.

Table 1 : Estimation of some initial plasma parameters for the incoming jet for the laboratory case and the astrophysical CTTS case.

	Laboratory	CTTS	
Incident jet	B-Field = 20T	B-Field = 5×10^{-3}T	B-Field = 5×10^{-2}T
Material	C_2H_3Cl (PVC)	H	H
Electronic density [$n.cm^{-3}$]	1.5×10^{18}	1.0×10^{11}	1.0×10^{11}
Temperature [eV]	30	2.6×10^{-1}	2.6×10^{-1}
Density [$g.cm^{-3}$]	8×10^{-6}	1.7×10^{-13}	1.7×10^{-13}
Speed accretion flow [$km.s^{-1}$]	600	500	500
Sound speed [$km.s^{-1}$]	38	6.47 | 118*	6.47 | 118*
Mach number	15.8	77.3 | 4.2*	77.3 | 4.2*
Alfven speed [$km.s^{-1}$]	1.96×10^{2}	3.46×10^{2}	3.46×10^{3}
Alfvenic Mach number	3.06	1.44	1.44×10^{-1}
Magnetic Reynolds	2.7	1.1×10^{8}	1.1×10^{8}
Magnetic diffusion time [ns]	71	17×10^{21}	17×10^{21}
β	4.5×10^{-2}	5	6×10^{-2}
Mean free path [mm]	2×10^{-2}	22.7	22.7

References

[1] B. Albertazzi et al., Science 346, 325 (2014)

[2] A. Ciardi et al., Phys. Rev. Lett. 110, 025002 (2013)

[3] U. Chaulagain et al., High Energy Density Physics (2015), http://dx.doi.org/10.1016/j.hedp.2015.01.003

[6] B. Albertazzi et al., Rev. Sci. Instru *84, 043505* (*2013*)

[5] S. Orlando et al., A&A 59, A127 (2013)

[6] Argiroffi, C., Maggio, A., & Peres, G. A&A 465, L5 (2007)